(2) Argon, A. S.; Cohen, R. E.; Gebizlioglu, O. S.; Schwier, C. E. *Adv. Polym. Sci.* **1983**, *52/53*, 275.
(3) Maglio, G.; Palumbo, R. The Role of Interfacial Agents in Polymer Blends. In *Polymer Blends*; Kryszewski, M., Galeski, A., Martuscelli, E., Ed.; Plenum: New York, 1982.
(4) Haws, J. R.; Wright, R. F. Block Polymers. Ch. 3 in *Handbook of Thermoplastic Elastomers*; Walker, B. M., Ed.; Krieger Pub. Co.: Melbourne, FL, 1986.
(5) Matzner, M.; Noshay, A.; McGrath, J. E. *Trans. Soc. Rheol.* **1977**, *21*, 273.
(6) Hadziioannou, G.; Skoulios, A. *Macromolecules* **1982**, *15*, 267.
(7) Cantor, R. *Macromolecules* **1981**, *14*, 1186.
(8) Hashimoto, T.; Shibayama, M.; Kawai, H. *Macromolecules*, **1980**, *13*, 1237.
(9) Han, C. C., private communication. See also: Mathushita, Y.; Nakao, Y.; Saguchi, R.; Mori, K.; Choshi, H.; Muroga, Y.; Noda, I.; Nagasawa, M.; Chang, T.; Glinka, C. J.; Han, C. C. *Macromolecules* **1988**, *21*, 1802.
(10) de Gennes, P.-G. *Scaling Concepts in Polymer Physics*; Cornell: Ithaca, NY, 1979.
(11) Edwards, S. F. *Proc. Phys. Soc.* **1965**, *85*, 613. Edwards, S. F. The Configurations and Dynamics of Polymer Chains In *Molecular Fluids*; Balian, R., Weill, G., Eds.; Gordon and Breach: London, 1976.
(12) Doi, M.; Edwards, S. F. *The Theory of Polymer Dynamics*; Clarendon Press: Oxford, 1986.
(13) Semenov, A. N. *Zh. Exp. Theor. Phys.* **1985**, *88*, 1242; translated in *Sov. Phys. JETP* **1985**, *61*, 733.
(14) Milner, S. T.; Witten, T. A.; Cates, M. E. *Europhys. Lett.* **1988**, *5*, 413. Milner, S. T.; Witten, T. A.; Cates, M. E. *Macromolecules* **1988**, *21*, 2610.
(15) Helfand, E.; Wasserman, Z. R. *Macromolecules* **1978**, *5*, 960.
(16) Viovy, J. L.; Gelbart, W. M.; BenShaul, A. *J. Chem. Phys.* **1987**, *87*, 4114.
(17) Leibler, L. *Makromol. Chem.-Macromol. Symp.* **1988**, *16*, 1.
(18) Milner, S. T.; Wang, Z.-G.; Witten, T. A. *Macromolecules* **1989**, *22*, 489.
(19) Noolandi, J.; Hong, K. M. *Macromolecules* **1982**, *15*, 482.
(20) Graessley, W. W. *Adv. Polym. Sci.* **1974**, *16*, 1.
(21) de Gennes, P.-G. *J. Chem. Phys.* **1971**, *55*, 572.
(22) Carella, J. M.; Gotro, J. T.; Graessley, W. W. *Macromolecules* **1986**, *19*, 659.
(23) The relaxation process is very similar to that postulated for star molecules in ref 12, p 280. As in the star system, the viscosity η is not simply the rubber modulus G_0 times the terminal relaxation time τ. Rather, only a small portion of order N/k^2G_0 of the initial stress requires such a time to relax. Thus this mechanism gives $\eta \sim G_0\tau N/k^2$.
(24) Graessley, W. W. *Adv. Polym. Sci.* **1982**, *47*, 67. Marrucci, G. In *Advances in Transport Processes*; Mujumdar, A. S., Mashelkar, R. A., Eds.; Wiley: New York, 1985; Vol. 5.
(25) Grest, G. S.; Kremer, K.; Milner, S. T.; Witten, T. A. *Macromolecules* **1989**, *22*, 1904.
(26) We assume that the solvent casting procedure of ref 8 produces the equilibrium domain thickness. The equilibrium thickness should in any case be larger than the measured one.
(27) Lin, Y.-H. *Macromolecules* **1987**, *20*, 3080.
(28) Taunton, H. J.; Toprakcioglu, C.; Fetters, L. J.; Klein, J. *Nature* **1988**, *332*, 712.

Molecular Dynamics in Bulk *cis*-Polyisoprene As Studied by Dielectric Spectroscopy

Diethelm Boese* and Friedrich Kremer

Max-Planck-Institut für Polymerforschung, Postfach 3148, 6500 Mainz, FRG.
Received May 23, 1989; Revised Manuscript Received July 17, 1989

ABSTRACT: Dielectric spectroscopy from 10^{-1} to 10^9 Hz was used to investigate bulk amorphous *cis*-polyisoprenes with different molecular weights having narrow molecular weight distributions. A molecular weight dependent normal-mode relaxation process due to reorientation of the end-to-end vector as well as a molecular weight independent segmental-mode process caused by local chain motions were observed. The relaxation time for the normal-mode process exhibits a molecular weight dependence that can be described below a critical molecular weight, M_c ($=10^4$), according to the Rouse theory; but above M_c the relaxation time follows the 3.7 power of M_w, which is explicable with the reptation theory. Both processes were analyzed in terms of dipole–dipole correlation functions and reveal a Kohlrausch–Williams–Watts (KWW) type of relaxation behavior. The nonexponential decay is explained with the cooperative nature of motions in the bulk amorphous state. The stretched exponential β_{KWW} for the normal-mode process depends on the chain length whereas it remains constant for the segmental process. The results are in agreement with new theoretical and computational approaches.

I. Introduction

It is well established[1,2] that most dipolar amorphous polymers give rise of multiple dielectric relaxation processes. Among them, the well-known α and β processes are often found. Their frequency–temperature locations are essentially independent of molecular weight.[3]

From a variety of macromolecules only a few reveal a low-frequency relaxation, which is strongly dependent on molecular weight.[4] The first dielectric investigation in the bulk amorphous state for poly(propylene oxide), which contains both a "fast" α process and a "slow" molecular weight dependent process, was carried out by Baur and Stockmayer.[5,6] The latter process was interpreted with the Rouse–Zimm theory for unentangled polymer chains.[7,8] For the entangled state of poly(propylene oxide), the experimental results of Beevers et al.[9] were compared with the predictions of the models for reptational motions of chains, as proposed by de Gennes[10] and Doi and Edwards.[11] Adachi and Kotaka[12-16] studied *cis*-polyisoprene in its undiluted state and observed two relaxation regions, as in the case for poly(propylene oxide). Because of the asymmetry in the chemical structure of *cis*-polyisoprene, the polymer has components of the dipole moment both parallel and perpendicular to the chain contour (Figure 1). Therefore, *cis*-polyisoprene exhibits a

0024-9297/90/2223-0829$02.50/0 © 1990 American Chemical Society

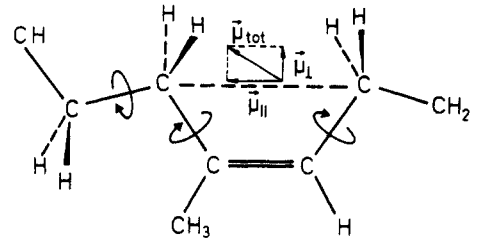

Figure 1. Chemical structure and dipole moments of the monomer unit of *cis*-polyisoprene.

dielectric normal-mode process caused by the parallel dipole moment as well as an α segmental-model process, which has its origin in local motions of the perpendicular dipole moment. For samples with molecular weights below the critical molecular weight, M_c (=10^4), the relaxation time for the normal-mode process was found to be proportional to $M_w^{2.0}$, in agreement with the Rouse theory,[7] and above M_c it followed the 3.7 power of M_w, which has been explained semiquantitatively by the tube theory.[10] Linear flexible polymers having moments aligned in the direction parallel to the chain contour show a dielectric relaxation due to reorientation of the end-to-end vector $\mathbf{r}$, which gives rise for a dipole correlation function as proposed earlier by Stockmayer.[6,17,18] For dipole moments perpendicular to the chain contour, Williams et al.[19-21] introduced molecular correlation functions, describing the time-dependent dipole moment correlations along a chain.

In this paper the dielectric properties of bulk *cis*-polyisoprene, having narrow molecular weight distribution, were reexamined, and its molecular dynamics were analyzed in terms of correlation functions comprising both the normal- and the segmental-mode relaxation. The results are compared with new theoretical and computational approaches.

II. Theory

The complex dielectric permittivity $\epsilon^*(\omega) = \epsilon'(\omega) - i\epsilon''(\omega)$ of a macroscopic system is given by the one-sided Fourier or pure imaginary Laplace transform of the time derivative of the normalized response function, $\Phi(t)$, for the dielectric polarization of the system[19-24]

$$\frac{\epsilon^*(\omega) - \epsilon_\infty}{\epsilon_{st} - \epsilon_\infty} = \int_0^\infty \exp[-i\omega t]\left[-\frac{d\Phi(t)}{dt}\right] dt \qquad (1)$$

where ϵ_{st} and ϵ_∞ are the limiting low- and high-frequency permittivities, respectively. The response function $\Phi(t)$ can be decomposed into contributions of dipole moment components parallel, μ'', and perpendicular, $\mu^\perp$, to the chain contour (ref 15, Appendix). The parallel components correspond to the end-to-end vector motion $\sum_j\sum_l\langle\mu_{ij}''(0)\,\mu_{il}(t)\rangle = \mu^2\langle\mathbf{r}_i(0)\,\mathbf{r}_i(t)\rangle$. Thus $\Phi(t)$ is written as

$$\Phi(t) = \frac{\mu^2\langle\mathbf{r}_i(0)\,\mathbf{r}_i(t)\rangle + \sum_j\sum_l\langle\mu_{ij}^\perp(0)\,\mu_{il}^\perp(t)\rangle}{\mu^2\langle\mathbf{r}_i(0)\,\mathbf{r}_i(0)\rangle + \sum_j\sum_l\langle\mu_{ij}^\perp(0)\,\mu_{il}^\perp(0)\rangle} \qquad (2)$$

where μ is the constant having the meaning of the parallel dipole moment per unit contour length and $\langle\mathbf{r}_i(0)\,\mathbf{r}_i(t)\rangle$ is the end-to-end vector autocorrelation function for the chain i at time t. The second term of eq 2 is simply reduced to the autocorrelation function of the perpendicular dipole moment component representing segmental motions. For detailed analysis the reader is referred to Williams et al.[24,25]

Since the relaxation times for the two components of $\Phi(t)$ are well separated in time domain, the individual autocorrelation functions are accessible and can be calculated.[15] For nonentangled polymers, $\langle\mathbf{r}_i(0)\,\mathbf{r}_i(t)\rangle$ is given by the Rouse–Zimm theory.[7,8] According to the free-draining model proposed by Rouse,[7] the correlation function is given by

$$\langle\mathbf{r}(0)\,\mathbf{r}(t)\rangle/\langle\mathbf{r}^2\rangle = (8/\pi^2)\sum(1/p^2)\exp(-t/\tau_p) \qquad (3)$$

$$\tau_p = \frac{\zeta N^2 b^2}{3\pi^2 k_B T p^2} \qquad p = 1, 3, 5, \ldots \qquad (4)$$

where τ_p is the relaxation time for the pth normal mode, ζ the friction coefficient per monomer unit, and N the number of chain segments with bond length b. Since N is proportional to the molecular weight M the Rouse theory predicts for the longest relaxation time $\tau_1 \propto M^2$.

For entangled polymer systems the tube model derived by de Gennes[10] predicts that the correlation function for the end-to-end vector is given by the same form as eq 3. The maximum relaxation time τ_d for the tube disengagement process or reptation process is different from τ_1 in the Rouse theory. The ratio between τ_d and τ_1 is written as

$$\tau_d/\tau_1 = 3L/b \qquad (5)$$

where L is the contour length of the primitive chain. This model predicted the $M^{3.0}$ dependence of τ_d.

Experiments on high molecular melts are in qualitative agreement with the predictions of the reptation theory but yield a slightly higher exponent of 3.4, e.g., for the zero shear viscosity, which is proportional to τ_d. Consequently, the validity of the concept has been questioned, and several new theoretical and computational approaches to polymer dynamics have been developed.[26-30]

Among them, the computer simulation of Pakula and Geyler,[31,32] involving cooperative motions in condensed polymer systems, is in agreement with the predictions of Rouse and reptation for the center-of-mass motion but reveals nonexponential correlation functions, which are of interest for the further analysis.

It is beyond the scope of this present paper to discuss in detail the various models describing the molecular dynamics of segmental relaxation modes. Most such studies proceed by evaluating the autocorrelation function of the second term in eq 2. Following the approach of Cook et al.,[20] who do not consider the detailed mechanical motions of chains, no specific model for chain dynamics or structural relaxation has been preferred. For details the reader is referred to selected papers and reviews.[3,24,33]

III. Experimental Section

Linear *cis*-polyisoprene were prepared by anionic polymerization in hexane at 303 K with *sec*-butyllithium as initiator to produce linear polymers with narrow molecular weight distribution. Weight-average molecular weights, M_w, were determined by low-angle light scattering and osmometry, respectively. Gel permeation chromatography (GPC) was employed to determine the molecular weight distribution, M_w/M_n. The microstructure of *cis*-polyisoprene was analyzed using ^{13}C NMR.[34] The glass transition temperature, T_g, was determined from DSC at a heating rate of 20 K/min. The results are listed in Table I.

The dielectric measurements covered the frequency range from 10^{-1} to 10^9 Hz. Three different measurement systems were used: (1) A Solartron–Schlumberger frequency response analyzer FRA 1254, which was supplemented by using a high-impedance pream-

Table I
Characteristics of the *cis*-Polyisoprene Samples

code	$10^{-3}M_w$	M_w/M_n	T_g, K	microstructure, % of units		
				cis-1,4	*trans*-1,4	vinyl-3,4
PIP-01	1.1		200.0	74.6	18.4	7.0
PIP-05	5.1	1.03	207.1	78.8	17.9	3.3
PIP-08	8.4	1.03	211.2	78.8	17.9	5.0
PIP-12	11.7	1.03	211.2	78.2	17.9	3.9
PIP-13	13.5	1.03	211.5	77.9	18.1	4.0
PIP-14	14.2	1.03	213.4	79.1	15.2	5.7
PIP-17	17.2	1.02	213.1	76.4	17.8	5.8
PIP-38	38.2	1.03	213.1	78.6	16.7	4.7
PIP-65	65.0	1.03	213.2	78.5	16.7	4.8
PIP-97	97.0	1.02	213.2	75.7	18.1	6.2
PIP-130	130.0	1.05	213.0	77.4	18.1	4.5

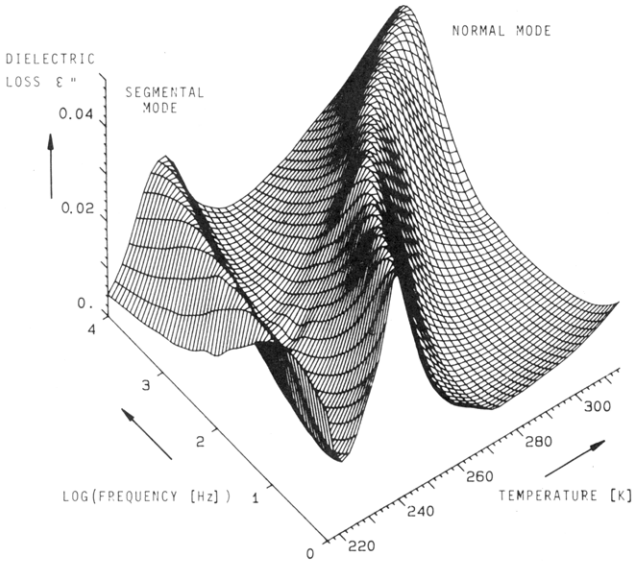

Figure 2. 3D representation of the frequency and temperature dependence of the dielectric loss, ϵ'', for *cis*-polyisoprene PIP-12.

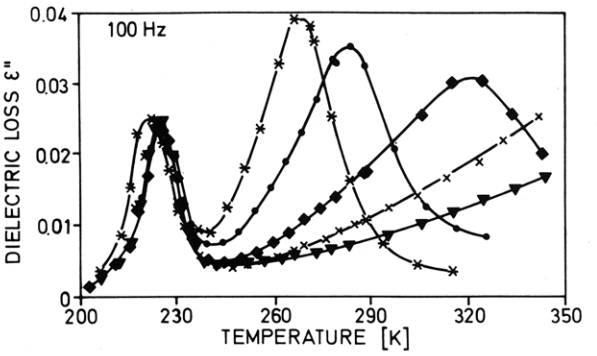

Figure 3. Temperature dependence of the dielectric loss, ϵ'', at 100 Hz for *cis*-polyisoprene with different molecular weights (see Table I): *, PIP-12; ●, PIP-17; ◆, PIP-38; ×, PIP-65; ▼, PIP-97.

plifier of variable gain,[35] covered the frequency range from 10^{-4} to 6×10^4 Hz. (2) In the audio frequency range (10–10^7 Hz) a Hewlett-Packard impedance analyzer 4192A was used. For both parts the sample material was kept between two condenser plates (gold-plated stainless steel electrodes; diameter 40 mm) with a separation of 150 μm, which was maintained by three fused silica pieces (area ≈2 mm²). (3) For the measurements between 10^6 and 10^9 Hz a Hewlett-Packard impedance analyzer 4191A was employed, which is based on the principle of a reflectometer. The sample was kept between two gold-plated stainless steel electrodes (diameter 6 mm) with a spacing of 50 ± 1 μm maintained by two fused silica fibers. The whole setup was mounted as a part of the inner conductor of the coaxial cell. All three arrangements were placed in custom-made cryostats, which allowed us to adjust the sample temperature between 100 and 500 K by use of a temperature-controlled nitrogen gas jet (stability ±0.02 K). For further details see ref 36.

IV. Results and Discussion

A. Dielectric Relaxation of Bulk Amorphous *cis*-Polyisoprene. The temperature and frequency dependence of the dielectric loss $\epsilon''(\nu)$ for undiluted PIP-12. Figure 2 shows a low-temperature process around 220 K just above the glass transition temperature (211 K) and hence assigned to the segmental-mode process. It originates from local motions of the perpendicular dipole moment. The positions of the loss maxima arising from segmental motions are almost independent of molecular weight (Figure 3). In contrast, the relaxation process above 250 K exhibits a pronounced dependence on molecular weight; it shifts to higher temperatures with increasing molecular weight (Figure 3). This is characteristic for a normal-mode process, which corresponds to motions of the entire chain caused by dipole components parallel to the backbone.[12-14]

In a region $T_g + 10\ \text{K} < T < T_g + 100\ \text{K}$ the applicability of the Williams–Landel–Ferry (WLF) equation[37] to describe the temperature dependence of the dynamic response of a system is generally accepted.[38] The temperature dependence of the relaxation rate ν_{max} at maximum $\epsilon''_{max}(\nu)$ is expressed by

$$\log \frac{\nu_{max}}{\nu_0} = \frac{C_1(T - T_0)}{C_2 + T - T_0} \tag{6}$$

where T_0 is a reference temperature, ν_0 is its corresponding relaxation rate, and C_1 and C_2 are fitting parameters. The values of these parameters are calculated via nonlinear least-squares fit with $T_0 = 250$ K for the segmental-mode process and $T_0 = 300$ K for the normal-mode process, respectively. The results are listed in Table II and plotted in Figure 4a,b. To compare the obtained fit parameters with the values of Adachi and Kotaka[13] who use the Vogel–Fulcher–Tamman (VFT) equation[39-41]

$$\log \nu_{max} = A - B/(T - T_\infty) \tag{7}$$

(where A, B, and T_∞ are parameters), the activation parameters $B = C_1C_2$ and $T_\infty = T_0 - C_2$[38] have been calculated; they are in agreement for selected samples (Table III). As presented in Table II and plotted in Figure 4a,b, the relaxation rates for the segmental process and hence the activation parameters are almost independent of molecular weight except for very low molecular weights. In contrast, the relaxation rate for the normal mode shows a strong dependence on the molecular weight and demonstrates a weaker temperature dependence.

B. Distribution of Relaxation Times for the Segmental- and Normal-Mode Process. For samples hav-

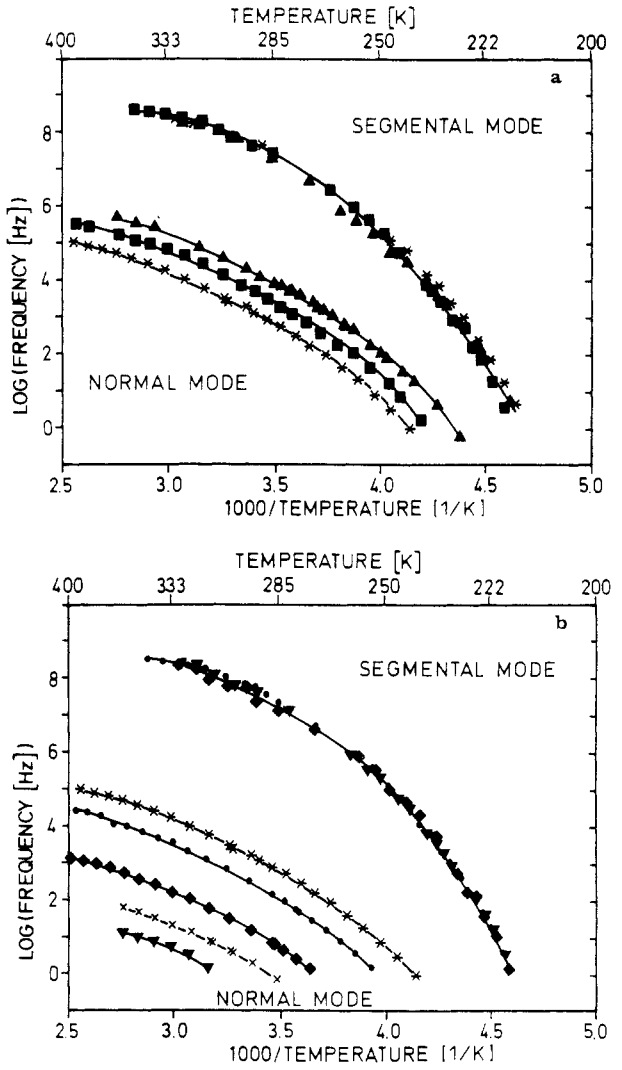

Figure 4. (a) Activation plot for the segmental mode and the normal mode of *cis*-polyisoprene samples with molecular weights of $M_w < M_c$: ▲, PIP-05; ■, PIP-08; *, PIP-12. The solid lines represent the WLF fit with the fit parameters given in Table II. (b) Activation plot for the segmental mode and the normal mode of *cis*-polyisoprene samples with molecular weights of $M_w > M_c$: *, PIP-12; ●, PIP-17; ◆, PIP-38; ×, PIP-65; ▼, PIP-97. The solid lines represent the WLF fit with the fit parameters given in Table II.

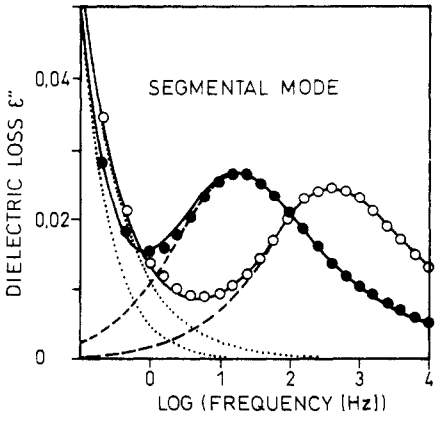

Figure 5. Fit of ϵ'' for the segmental-mode process of PIP-17 using the Havriliak–Negami equation (eq 8). Experimental data are given for T = 222.3 K (●) and for T = 229.5 K (○). The dotted curve represents the conductivity contribution according to eq 9 and the dashed curve the relaxation contribution to ϵ''. The fit parameters are shown in Table IV.

Table II
WLF Parameters C_1, C_2, and ν_0 Determined by Equation 6 for the Segmental- and Normal-Mode Processes

	segmental mode, T_0 = 250 K			normal mode, T_0 = 300 K		
code	C_1	C_2, K	$10^{-5}\nu_0$, Hz	C_1	C_2, K	ν_0, Hz
PIP-01				4.0	151.6	2.0×10^6
PIP-05	5.7	80.0	1.2	4.0	133.9	3.1×10^4
PIP-08	5.7	70.0	2.1	4.3	136.2	7.4×10^3
PIP-12	5.8	76.0	2.5	4.2	132.3	2.0×10^3
PIP-13	5.8	74.3	2.2	4.2	128.8	1.3×10^3
PIP-14	6.0	69.7	1.5	4.4	130.5	8.1×10^2
PIP-17	6.1	70.9	1.4	4.4	129.5	3.9×10^2
PIP-38	6.0	71.2	1.6	4.2	119.9	2.2×10^1
PIP-65	6.1	73.4	1.7	3.6	97.5	3.1
PIP-97	6.1	70.9	1.4	0.9	57.9	0.02
PIP-130	6.1	72.5	1.6			

Table III
VFT Parameters Calculated According to Reference 38 for the Segmental- and Normal-Mode Processes[a]

	segmental mode		normal mode	
code	B, K	T_∞, K	B, K	T_∞, K
PIP-05	456.0 (422.5)	170.0 (173.8)	535.6 (530.2)	166.1 (168.4)
PIP-12	440.8 (413.0)	174.0 (174.6)	547.2 (510.2)	169.7 (169.5)
PIP-38	427.2 (438.3)	178.8 (175.9)	503.6 (495.0)	180.1 (175.9)

[a] The values in parentheses are drawn from Adachi and Kotaka[13] for samples having similar molecular weight: M_w = 5000, M_w = 11 000, and M_w = 42 000, respectively.

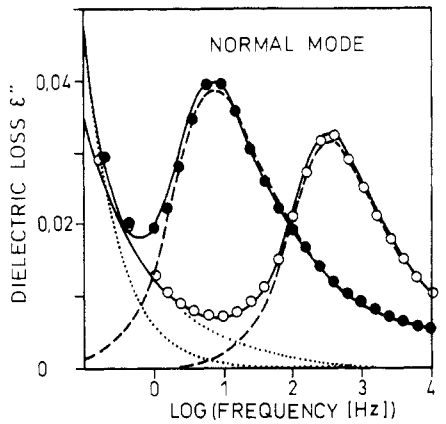

Figure 6. Fit of ϵ'' for the normal-mode process of PIP-17 using the Cole–Davidson approach[45] for T = 263.9 K (●) and T = 297.8 K (○). The dotted curve represents the conductivity contribution according to eq 9 and the dashed curve the relaxation contribution of ϵ''. The fit parameters are listed in Table IV.

ing molecular weights $M_w \geq 8000$, it is possible to analyze the two relaxation processes individually. For this reason the loss curves are resolved into the contributions of the normal- and segmental-mode process arising from their different temperature dependence (Figures 5 and 6).

Since the loss curves were broad and asymmetric, the Havriliak–Negami (HN) function was used to fit the data[42,43]

$$\epsilon^*(\omega) = \epsilon_\infty + \frac{\Delta\epsilon_{HN}}{(1 + (i\omega\tau_{HN})^\alpha)^\gamma} \tag{8}$$

where ϵ_∞ is the limiting low-frequency permittivity and $\Delta\epsilon_{HN} = \epsilon_{st} - \epsilon_\infty$ denotes the relaxation strength. α is a parameter characterizing a symmetrical broadening of distribution of relaxation times, and γ characterizes an asymmetrical broadening ($0 < \alpha, \gamma \leq 1$). This function is a generalization of the well-known Cole–Cole (CC) and Cole–Davidson (CD) descriptions.[44,45]

Table IV
Parameters of the HN Equation for the Segmental- and Normal-Mode Processes for PIP-17[a]

T, K	$\Delta\epsilon_{HN}$	α	γ	τ_{HN}, s	σ_0, Ω cm	s
			Segmental Mode			
222.3	0.117	0.70	0.50	2.2×10^{-2}	2.8×10^{-11}	1.0
224.3	0.115	0.68	0.51	8.7×10^{-3}	3.5×10^{-11}	1.0
226.4	0.114	0.65	0.55	3.0×10^{-3}	4.2×10^{-11}	1.0
229.5	0.111	0.65	0.56	8.8×10^{-4}	6.5×10^{-11}	0.7
240.4	0.097	0.64	0.59	2.2×10^{-5}		
244.4	0.097	0.64	0.68	8.5×10^{-6}		
253.9	0.091	0.62	0.66	9.0×10^{-7}		
			Normal Mode			
263.9	0.127	1.0	0.38	4.6×10^{-2}	3.4×10^{-11}	0.9
272.5	0.118	1.0	0.40	1.2×10^{-2}	4.0×10^{-11}	1.0
283.7	0.105	1.0	0.42	3.5×10^{-3}	6.0×10^{-11}	1.0
297.7	0.096	1.0	0.44	9.4×10^{-4}	7.0×10^{-11}	0.5
324.4	0.085	1.0	0.45	1.3×10^{-4}		
341.7	0.082	1.0	0.45	6.1×10^{-5}		
359.4	0.078	1.0	0.44	3.2×10^{-5}		
376.6	0.077	1.0	0.44	2.0×10^{-5}		

[a] Havriliak-Negami parameters $\Delta\epsilon_{HN}$, α, γ, and τ_{HN} from the fit of eq 8 to ϵ'' data. σ_0 and s according to eq 9.

The steep rise at low frequencies (Figures 5 and 6) is caused by frequency-dependent electrical conductivity within the sample

$$\epsilon''(\omega) = \frac{\sigma_0}{\epsilon_0(2\pi\nu)^s} \tag{9}$$

where σ_0 and s are fitting parameters.[46] σ_0 describes the contribution of mobile charge carriers to the dielectric loss $\epsilon''(\omega)$, and ϵ_0 denotes the permittivity of free space. Values of $0.5 \leq s \leq 1$ in the exponent are found, indicating that the conductivity orginates from the hopping process. Figures 5 and 6 show that the HN function gives a good fit to the experimental data; the fit parameters for one representative sample (PIP-17) are combined in Table IV.

It is seen from Table IV that the shape parameters α and γ for the segmental-mode process show systematic deviation. With increasing temperature, α decreases slightly whereas the γ parameter rises to higher values. This is observed for all samples under study and is in agreement with earlier investigations.[47-49] For the normal-mode process the HN function is reduced to the Cole-Davidson function (CD) with $\alpha = 1.0$. The CD function can be applied to all samples with $M_w \geq 8000$, indicating that the normal-mode process has a narrower relaxation time distribution than the segmental-model process.

C. Correlation Function for the Segmental- and Normal-Mode Process. The application of eq 1 states that the complex dielectric permittivity $\epsilon^*(\omega) = \epsilon'(\omega) - i\epsilon''(\omega)$ is given by the one-sided Fourier transform of the quantity $[-d\Phi(t)/dt]$. Since $\epsilon'(\omega)$ and $\epsilon''(\omega)$ are related to each other via a Kramers-Kronig relation, the further evaluation concentrates only on $\epsilon''(\omega)$ to extract $\Phi(t)$ from measured quantities. This is done by a half-sided cosine transformation:

$$\Phi(t) = \frac{2}{\pi}\int_0^\infty \frac{\epsilon''(\omega)}{\epsilon_{st} - \epsilon_\infty}\frac{\cos \omega t}{\omega}\, d\omega \tag{10}$$

In order to calculate $\Phi(t)$ from eq 10 by numerical integration, the functional form of the HN description was used to evaluate $\epsilon''(\nu)$ data over the entire relaxation range. This proceeding has the advantage to calculate the correlation function by an analytical and well-known equation. Furthermore, it provides the possibility of employing the HN parameters published by Adachi and Kotaka[13] and of comparing $\Phi(t)$ directly with our results.

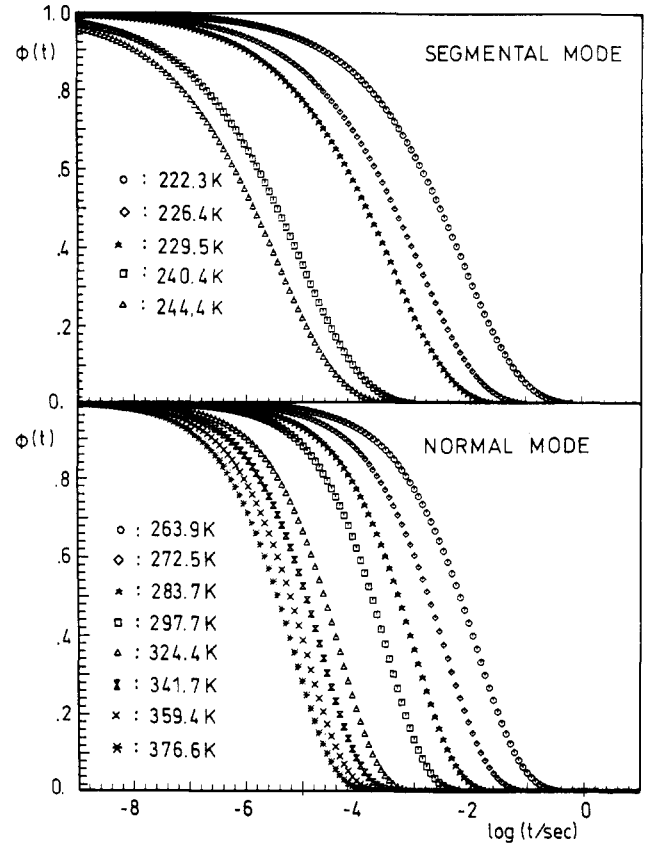

Figure 7. Normalized correlation function for the segmental mode and normal mode of PIP-17 calculated according to eq 10 using the HN parameters are given in Table IV. The resulting β parameters are shown in Table V.

To the resulting correlation functions (Figure 7), the empirical relation as given by the Kohlrausch-Williams-Watts (KWW) function

$$\Phi(t) = \exp\left[-\left(\frac{t}{\tau_{KWW}}\right)^\beta\right] \quad 0 < \beta \leq 1 \tag{11}$$

is fitted. The β parameter describes the nonexponential chracter of the correlation function and τ_{KWW} is the time at which $\Phi(t)$ falls to its $1/e$ point.[19,20]

From the determined parameters the mean relaxation time can be obtained via

$$\langle\tau_{KWW}\rangle = (\tau_{KWW}/\beta)\Gamma(1/\beta) \tag{12}$$

Table V
KWW Parameters for Both Segmental- and Normal-Mode Processes of the Representative PIP-17[a]

T, K	β	τ_{KWW}, s	$\langle\tau_{KWW}\rangle$, s	$\langle\tau\rangle$, s
		Segmental Mode		
222.3	0.40	7.1×10^{-3}	1.6×10^{-2}	8.4×10^{-3}
224.3	0.40	2.8×10^{-3}	6.2×10^{-3}	3.3×10^{-3}
226.4	0.39	1.1×10^{-3}	2.5×10^{-3}	1.2×10^{-3}
229.5	0.39	3.5×10^{-4}	8.0×10^{-4}	4.1×10^{-4}
240.4	0.39	9.2×10^{-6}	2.1×10^{-5}	1.4×10^{-5}
244.4	0.39	3.5×10^{-6}	8.0×10^{-6}	3.2×10^{-6}
253.9	0.39	4.8×10^{-7}	1.1×10^{-6}	4.1×10^{-7}
		Normal Mode		
263.9	0.54	1.3×10^{-2}	2.3×10^{-2}	2.0×10^{-2}
272.5	0.56	3.5×10^{-3}	5.8×10^{-3}	5.5×10^{-3}
283.7	0.58	1.1×10^{-3}	1.7×10^{-3}	1.7×10^{-3}
297.7	0.61	3.2×10^{-4}	4.7×10^{-4}	4.6×10^{-4}
324.4	0.61	4.5×10^{-5}	6.6×10^{-5}	6.4×10^{-5}
341.7	0.61	2.1×10^{-5}	3.1×10^{-5}	3.3×10^{-5}
359.4	0.61	1.1×10^{-5}	1.6×10^{-5}	1.6×10^{-5}
376.6	0.60	6.8×10^{-6}	1.0×10^{-6}	8.5×10^{-6}

[a] β and τ_{KWW} parameters from the fit of $\phi(t)$ from eq 10 to KWW representation of eq 11. $\langle\tau_{KWW}\rangle$ is according to eq 12 and $\langle\tau\rangle$ is obtained from $\langle\tau\rangle = (2\pi\nu_{max})^{-1}$.

where Γ denotes the Γ function.[50] The results for the representative PIP-17 are listed in Table V.

Segmental Dipole–Dipole Correlation Function. The β parameter for the segmental process is found to be constant over the entire temperature range. This holds for all samples with $8000 \leq M_w \leq 97\,000$ and reveals a mean β value of 0.40 ± 0.02 whereas the α and γ values from the HN equation (Table IV) show a systematic temperature deviation. This is in close agreement with the results discussed in a previous paper;[48,49] the fit quality of the HN and KWW representation was found to be comparable.[48] The related KWW parameters at 273 K for samples used by Adachi and Kotaka yield:

code	β	$10^8\tau_{KWW}$, s
PI-05	0.39	1.3
PI-14	0.39	1.8
PI-32	0.39	2.0
PI-53	0.39	1.6

These values are obtained from the HN parameters in Table III of ref 16. The mean β value is in agreement within its error bars with our results (Table V).

The nonexponential decay of the correlation function for the segmental-mode process has been explained with the cooperative nature of motions in the amorphous rubbery state.[25] Skinner[51,52] has worked out a kinetic Ising model of "spin" flips resulting in a diffusionlike motion of defects. These produce a correlation function of the KWW form with β_{KWW} in the range of 0.74–0.50. Fredrickson and Brawer[53] developed a kinetic Ising model with single-spin-flip dynamics and highly cooperative flip rates. Their approach leads to a non-Arrhenius temperature dependence of the mean relaxation time as well as a nonexponential decay of correlation functions. It was shown that the time correlation functions can be accurately fit to the KWW expression. As noted in the theoretical part and briefly summarized above, quite different models may lead to correlation functions of the KWW type. But in each case the function results from the cooperative nature of the developed model.

End-to-End Vector Correlation Function. As seen in Table V the β value for the normal-mode process decreases with decreasing temperature. This behavior is observed for molecular weights between 8000 and 97 000.

Table VI
KWW Parameters for the Normal-Mode Process at $T = 322 \pm 3$ K for Various Samples

code	T, K	β	τ_{KWW}, s	$\langle\tau_{KWw}\rangle$, s	$\langle\tau\rangle$, s
PIP-08	324.4	0.65	3.0×10^{-6}	4.1×10^{-6}	3.9×10^{-6}
PIP-12	324.8	0.63	1.1×10^{-5}	1.5×10^{-5}	1.6×10^{-5}
PIP-13	319.9	0.61	1.9×10^{-5}	2.8×10^{-5}	2.8×10^{-5}
PIP-14	320.3	0.61	3.4×10^{-5}	5.0×10^{-5}	5.3×10^{-5}
PIP-17	324.4	0.61	4.5×10^{-5}	6.6×10^{-5}	6.4×10^{-5}
PIP-38	324.4	0.54	7.5×10^{-4}	1.3×10^{-3}	1.3×10^{-3}
PIP-65	323.8	0.54	6.0×10^{-3}	1.0×10^{-2}	1.0×10^{-2}
PIP-97	325.1	0.52	2.0×10^{-2}	3.7×10^{-2}	3.9×10^{-2}

For the further analysis only those values are discussed where β is nearly independent of temperature and where the relaxation process is far from the glass transition region. With a view to compare our results with the Adachi and Kotaka values, measurements at 320 + 4 K are evaluated (Table VI). As expected[54] the response function and consequently the β values exhibit a molecular weight dependence. With increasing molecular weight the β parameter decreases slightly. A similar dependence was observed by Adachi and Kotaka[14] where they evaluated Cole–Davidson distribution parameters from master plots with a reference temperature of 320 K. The Cole–Davidson parameters for bulk *cis*-polyisoprene with M_w = 102 000, M_w = 42 000, and M_w = 11 000 are determined to be 0.22, 0.25, and 0.40, respectively. The conversion into the KWW β value using the Lindsey–Patterson equation[50] yields 0.36, 0.38, and 0.53, respectively. These values are much smaller than those listed in Table VI due to broad molecular weight distribution M_w/M_n ranging from 1.17 to 1.34. The decrease in γ with increasing molecular weight was closely related to the "entanglement effect".[13] An interesting approach we used to explain our experimental data has been developed by Pakula and Geyler[31,32] who carried out computer simulations for cooperative relaxations in condensed macromolecular systems. The conformational relaxation in a system of linear chains is characterized by the end-to-end vector autocorrelation function which follows the stretched exponential or KWW form. The model takes into consideration a large variety of cooperative rearrangements as well as a large variety of local structural situations. This results in a broad spectrum of relaxation times and consequently leads to the nonexponential decay of the end-to-end vector autocorrelation function. When our results are compared with those from the simulation,[31] the characteristic ratio C_∞ = 5.1 for *cis*-polyisoprene with about 70% cis-1,4, 23% trans-1,4, and 7% 3,4 units was used.[55] The predicted β values are

$$M_w = 7400 \rightarrow \beta = 0.68$$

$$M_w = 14\,700 \rightarrow \beta = 0.62$$

$$M_w = 29\,600 \rightarrow \beta = 0.57$$

The parameters are in good agreement with the experimental results (Table VI). The nonexponential decay of the end-to-end vector autocorrelation function that is observed experimentally and found in the computer simulations of Pakula and Geyler reflects mode–mode interactions due to intermolecular restraints of closed-packed chains. The close packing restricts motion of any element in the system until some other elements move with these elements cooperatively. Elementary cooperative motions are possible only along some structurally acceptable paths. This involves a strong hierarchy in degrees of freedom and makes fast and slow motions interdependent and dependent on the conformational state of the system.[32]

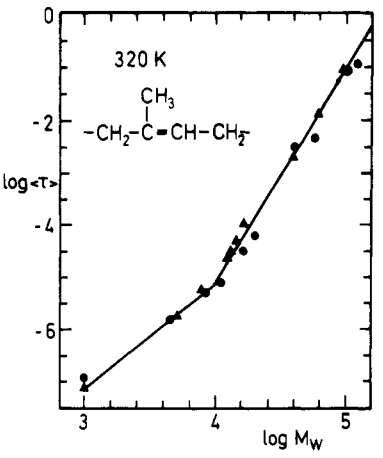

Figure 8. Dependence of the mean dielectric relaxation time, $\langle\tau\rangle = (2\pi\nu_{max})^{-1}$, on molecular weight, M_w, for the normal-mode process of *cis*-polyisoprene (▲) at 320 K; data are reported by Adachi and Kotaka (●) in ref 13.

It is remarkable that the mean relaxation times $\langle\tau_{KWW}\rangle$ correspond excellently to the mean relaxation times $\langle\tau\rangle$ obtained from the trivial relation $\omega_{max}\langle\tau\rangle = 1$, which is only valid for symmetric loss curves and fails in the strong asymmetric limit.

D. Molecular Weight Dependence of the Normal-Mode Relaxation Time. In Figure 8 the mean relaxation times for the normal-mode process are plotted against the molecular weight, indicating the predicted crossover from Rouse to reptation.[30]

The molecular weight dependence of the normal-mode relaxation time, $\langle\tau\rangle$, changes at the critical molecular weight M_c (=10^4) and is given by

$$\langle\tau\rangle \propto M^{2.0} \quad \text{for } M_w < M_c$$

$$\langle\tau\rangle \propto M^{3.7\pm0.1} \quad \text{for } M_w \geq M_c$$

As reviewed in the theoretical part these molecular weight dependences have been explained by the Rouse theory and by the reptation theory in its recent modifications.

V. Conclusions

1. The molecular weight dependence of the dielectric relaxation time for the normal-mode process below a critical molecular weight M_c (=10^4) obeys the Rouse theory where τ is proportional to $M^{2.0}$. Above M_c the normal-mode relaxation time is proportional to $M^{3.7}$, which is characteristic for entangled polymers. The segmental-mode process is found to be almost independent of molecular weight and hence to give similar activation parameters. This process is directly associated with the dynamic glass transition of the bulk polymer.

2. The distribution parameters α and γ of the Havriliak–Negami equation vary significantly with temperature for the segmental-mode process whereas the β parameter obtained from the Kohlrausch–Williams–Watts function remains constant over the whole temperature and molecular weight range, respectively. For the normal-mode process the Havriliak–Negami equation is reduced to the Cole–Davidson equation. The determined stretched exponential β depends on chain length and is in agreement with the results of computer simulation.

3. The nonexponential decay for both the segmental dipole–dipole correlation function and the end-to-end vector correlation function is explained by a relaxation behavior due to cooperative rearrangements.

Acknowledgment. D.B. is grateful to Prof. E. W. Fischer, Dr. T. A. Vilgis, Dr. T. Pakula, and S. Geyler for helpful discussions.

References and Notes

(1) McCrum, N. G.; Read, B. E.; Williams, G. *Anelastic and Dielectric Effects in Polymer Solids*; Wiley: London, 1967.
(2) Hedvig, P. *Dielectric Spectroscopy of Polymers*; Adam Hilger: Bristol, U.K., 1977.
(3) Williams, G. *Advances in Polymer Science*; Springer Verlag: Berlin, 1977; Vol. 33, p 59.
(4) Stockmayer, W. H.; Baur, M. E. *J. Am. Chem. Soc.* **1964**, *86*, 3485.
(5) Bauer, M. E.; Stockmayer, W. H. *J. Chem. Phys.* **1965**, *43*, 4319.
(6) Stockmayer, W. H. *Pure Appl. Chem.* **1967**, *15*, 247.
(7) Rouse, P. E. *J. Chem. Phys.* **1953**, *21*, 1272.
(8) Zimm, B. H. *J. Chem. Phys.* **1956**, *24*, 269.
(9) Beevers, M. S.; Elliot, D. A.; Williams, G. *Polymer* **180**, *21*, 13.
(10) de Gennes, P.-G. *J. Chem. Phys.* **1971**, *55*, 572.
(11) Doi, M.; Edwards, S. F. *J. Chem. Soc., Faraday Trans. 2* **1978**, *74*, 1789, 1802, 1818.
(12) Adachi, K.; Kotaka, T. *Macromolecules* **1984**, *17*, 120.
(13) Adachi, K.; Kotaka, T. *Macromolecules* **1985**, *18*, 466.
(14) Adachi, K.; Kotaka, T. *J. Mol. Liq.* **1987**, *36*, 75.
(15) Adachi, K.; Kotaka, T. *Macromolecules* **1988**, *21*, 157.
(16) Imanishi, Y.; Adachi, K.; Kotaka, T. *J. Chem. Phys.* **1988**, *89*, 7585, 7593.
(17) Jones, A. A.; Stockmayer, W. H. *Polym. Prepr. (Am. Chem. Soc., Div. Polym. Chem.)* **1974**, *15*, 16.
(18) Jones, A. A.; Stockmayer, W. H.; Molinari, R. J. *J. Polym. Sci. Symp.* **1976**, *54*, 227.
(19) Williams, G.; Watts, D. C. *Trans. Faraday Soc.* **1970**, *66*, 80.
(20) Cook, M.; Watts, D. C.; Williams, G. *Trans. Faraday Soc.* **1970**, *66*, 2503.
(21) Williams, G.; Watts, D. C.; Dev, S. B.; North, A. M. *Trans. Faraday Soc.* **1971**, *67*, 1323.
(22) Cole, R. H. *J. Chem. Phys.* **1965**, *42*, 637.
(23) Nee, T.-H.; Zwanzig, R. *J. Chem. Phys.* **1970**, *52*, 6353.
(24) Williams, G. *Chem. Rev.* **1972**, *72*, 55.
(25) Williams, G.; Cook, M.; Hains, P. J. *J. Chem. Soc., Faraday Trans. 2* **1972**, *68*, 1045.
(26) Kolinski, A.; Skolnick, J.; Yaris, R. *J. Chem. Phys.* **1987**, *86*, 1567.
(27) Skolnick, J.; Yaris, R.; Kolinski, A. *J. Chem. Phys.* **1988**, *88*, 1407, 1418.
(28) Hess, W. *Macromolecules* **1988**, *21*, 2620.
(29) Kavassalis, T. A.; Noolandi, J. *Macromolecules* **1988**, *21*, 2869.
(30) Kremer, K.; Grest, G. S.; Carmesin, I. *Phys. Rev. Lett.* **1988**, *61*, 566.
(31) Pakula, T.; Geyler, S. *Macromolecules* **1987**, *20*, 2909.
(32) Pakula, T.; Geyler, S. *Polymer Motion in Dense System*; Richter, D., Springer, T., Eds.; Springer Verlag: Berlin, 1988.
(33) Cole, R. H. *Molecular Liquids, Dynamics and Interactions*; Reidel: Dordrecht, The Netherlands, 1984.
(34) Sato, H.; Ono, A.; Tanaha, Y. *Polymer* **1977**, *18*, 580.
(35) Pugh, J.; Ryan, J. T. *IEEE Conf. Dielectr. Mater. Meas. Appl.* **1979**, *177*, 404.
(36) Kremer, F.; Boese, D.; Meier, G.; Fischer, E. W. *Progress in Colloid and Polymer Science*, in press.
(37) Williams, M. L.; Landel, R. F.; Ferry, J. D. *J. Am. Chem. Soc.* **1955**, *77*, 3701.
(38) Ferry, J. D. *Viscoelastic Properties of Polymers*; Wiley: New York, 1980.
(39) Vogel, H. *Z. Phys.* **1921**, *22*, 645.
(40) Fulcher, G. S. *J. Am. Ceram. Soc.* **1925**, *8*, 339.
(41) Tamman, G.; Hesse, W. *Z. Anorg. Allg. Chem.* **1926**, *156*, 245.
(42) Havriliak, S.; Negami, S. *J. Polym. Sci., Part C* **1966**, *14*, 99.
(43) Havriliak, S.; Negami, S. *Polymer* **1967**, *8*, 161.
(44) Cole, K. S.; Cole, R. H. *J. Chem. Phys.* **1941**, *9*, 341.
(45) Davidson, D. W.; Cole, R. H. *J. Chem. Phys.* **1951**, *19*, 1484.
(46) Mott, N. F.; Davis, E. A. *Electronic Processes in Non Crystalline Materials*; Clarendon Press: Oxford, U.K., 1979.
(47) Nozaki, S.; Mashimo, S. *J. Chem. Phys.* **1987**, *87*, 2271.
(48) Shioya, Y.; Mashimo, S. *J. Chem. Phys.* **1987**, *87*, 3173.
(49) Boese, D.; Momper, B.; Meier, G.; Kremer, F.; Hagenah, J.-U.; Fischer, E. W. *Macromolecules* **1989**, *22*, in press.
(50) Lindsey, C. P.; Patterson, G. D. *J. Chem. Phys.* **1980**, *73*, 3348.
(51) Skinner, J. L. *J. Chem. Phys.* **1983**, *79*, 1955.
(52) Budimir, J.; Skinner, J. L. *J. Chem. Phys.* **1985**, *82*, 5232.
(53) Fredrickson, G. H.; Brawer, S. A. *J. Chem. Phys.* **1986**, *84*, 3351.
(54) Block, H. *Advances in Polymer Science*; Springer Verlag: Berlin, 1979; Vol. 33, p 93.
(55) Hadjichristidis, N.; Zhongde, X.; Fetters, L. J.; Roovers, J. *J. Polym. Sci., Polym. Phys. Ed.* **1982**, *20*, 743.

Registry No. *cis*-Polyisoprene, 9003-31-0.